Separation of Pressure and Saturation effects using AVO 4D in Marlim Field

João Paulo Pereira Nunes, Petrobras, Brazil
Marcos Sebastião dos Santos, Petrobras, Brazil
Nier Maciel, Petrobras, Brazil
Alessandra Davolio, CGGVeritas, Brazil
Jean-Luc Formento, CGGVeritas, Brazil

Abstract

Using the method introduced by Landro (2001), it has been possible to study the pressure and saturation changes induced by production in the Marlim field, figure 1. This methodology does not make any assumption about production, requiring only petrophysical and seismic data covering the field of interest. Maps representing pressure and saturation changes are presented and also a section over one well, showing how these anomalies can be compared with flow simulator prediction. The main result obtained is a better understanding of the mechanism by which water saturation and effective pressure changes are created during field production.

Introduction

Since the beginning of the 4D monitoring technology, it is well known that seismic anomalies can be induced by pressure and/or saturation changes due to production, which may have the same impact on seismic differences. Thus, this kind of ambiguity can lead to incorrect understanding about the propagation and/or relevance of these different effects. The search for methods to discriminate pressure/saturation changes on seismic data has led to two main research lines: 1) Using prestack data, since the expression of saturation/pressure effects is different in near/far angles, see Landro (2001); 2) Using seismic attributes and pattern recognition schemes, MacBeth et al. (2006). In this work we apply the first methodology, requiring only seismic data and making no assumption about production.

Previous work on 4D AVO has been concentrated mainly in sandstone fields in North Sea, where, after petrophysical calibration, Landro reports the following relation between P/S and I/G for Gullfaks field:

$\Delta P = 23\Delta I - 35\Delta G$

$\Delta S = 8\Delta I + 8\Delta G$

Where P is effective pressure, S is saturation, G is the gradient and I is the intercept.

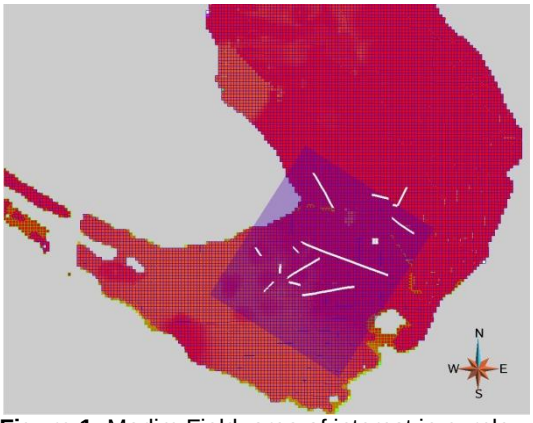

Figure 1: Marlim Field, area of interest in purple.

Method

Given a petrophysical calibration for the studied field, it is possible; by using first order approximations of the Smith & Gidlow AVO equations, to derive equations relating Pressure / Saturation changes with changes in intercept / gradient cubes, see Landro (2001).

Petrophysical calibration was performed using velocity and density core data measured by Petrobras Rock Physics Lab. Assuming a linear relationship for ΔRho versus saturation changes (Gassmann model) and quadratic relation for ΔVp and ΔVs versus effective pressure changes (figure 2), 6 coefficients can be estimated:

$\Delta Vp/Vp = k\alpha\, \Delta S + l\alpha\, \Delta P + m\alpha\, \Delta P^2$

$\Delta Vs/Vs = k\beta\, \Delta S + l\beta\, \Delta P + m\beta\, \Delta P^2$

$\Delta Rho/Rho = k\rho\, \Delta S$

Coefficients (mα, mβ…) obtained by these fitting are used to express numerically the relation between P/S and I/G for this reservoir

$\Delta P = 10\Delta I - 12.6\Delta G$

$\Delta S = 9.6\Delta I + 7.9\Delta G$

Comparing to Gullfaks, we observe that in Marlim field, gradient changes have a smaller effect on pressure and that saturation changes are slightly more sensible to intercept variations. Details about the relation between mα, mβ… and ΔP/ ΔS can be found in Landro's paper.

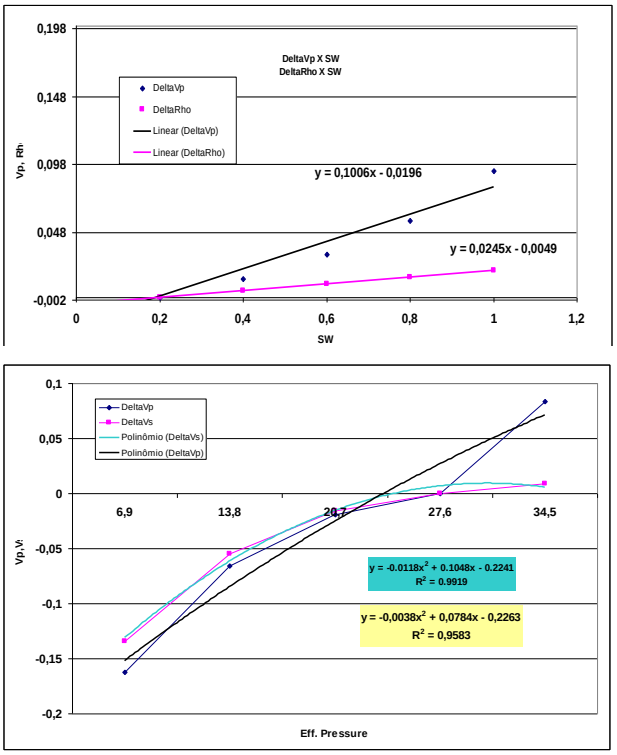

Figure 2:Petrophysical calibration. Vp and Rho versus SW (top). Vp and Vs versus eff. pressure (bottom).

The next step involves the evaluation of intercept/gradient attributes using the whole set of gathers (from 0 to 35 degrees) for both surveys (base and monitor). We employed some tools to stabilize the seismic response using processing algorithms such as Trimstatics and AVO stabilizer (Whitcombe et al., 2004), (figures 3-6), in order to improve signal/noise ratio for the difference cubes. Having the difference I/G cubes and the equations for P/S changes, we calculate maps of P/S changes in the top Marlim reservoir and correlate with well data.

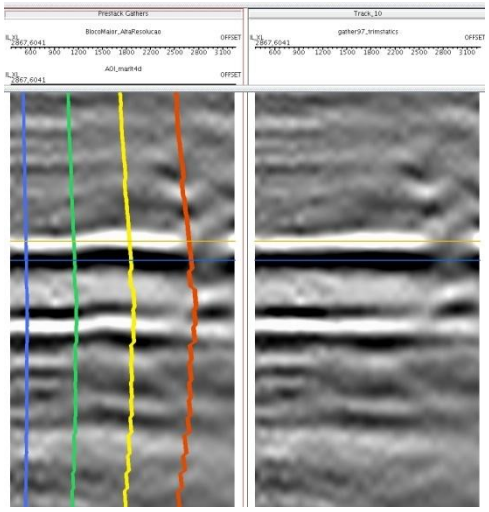

Figure 3: Gather before and after trimstatics.

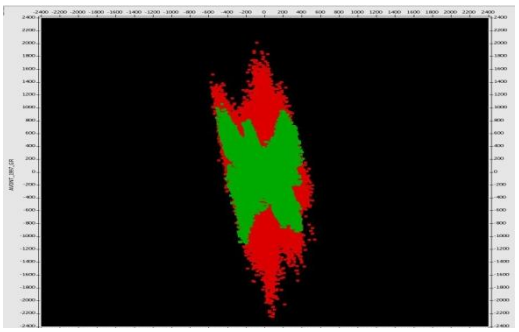

Figure 4: Stabilization in the Gradient X Intercept domain (in red).

The technique of AVO stabilization, described in Whitcombe paper (2004), allows noise suppression to be targeted at the noisiest direction in the AVO space. This provides light noise reduction to the intercept data and heavier suppression to the gradient data, as we can see on Figures 4-6. The resulting gradient data are more interpretable and better temporally aligned to the intercept data. Several attempts were performed to improve the AVO response comparing at each stabilization filter with the expected pressure and saturation changes.

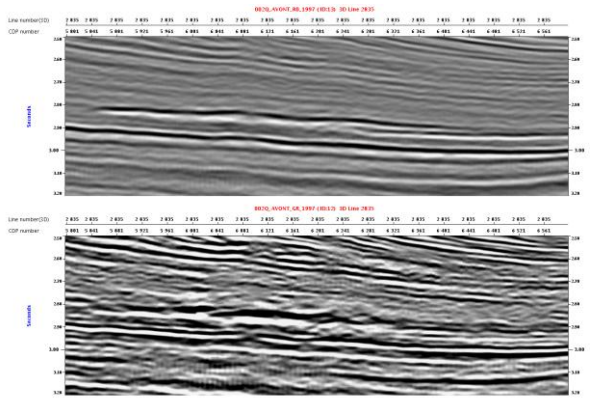

Figure 5: Arbitrary inline section of intercept (above) and gradient (below) before stabilization, time window around reservoir.

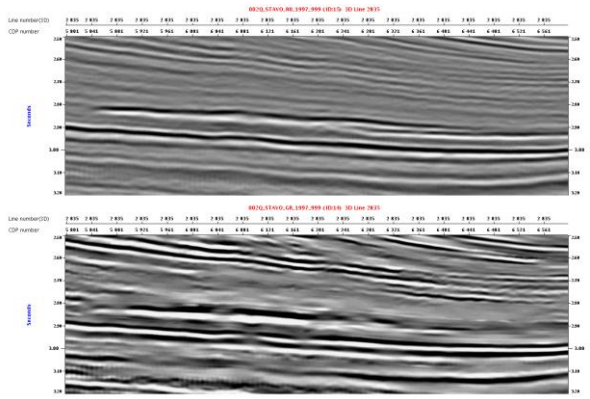

Figure 6: Same inline section of intercept (above) and gradient (below) after stabilization.

Results

The main results are the two cubes of pressure and saturation changes, which can be used to extract attributes over top reservoir horizon. These are the maps displayed in figures 8 and 10.

When we compare the maps of pressure and saturation changes with the difference of amplitude map (figure 7), we note that figures 8 and 10 present less noise. This is the result of the stabilization process applied to the AVO attributes (I and G).

As expected, the resulting maps have stronger geological character than the ones obtained by flow simulator only (figures 9 and 11), attention must be paid to the fact that at well locations both are consistent. The most drastic changes can be seen in the pressure map, where it is possible to see the underlying mechanism by which pressure increases are spreading (or not).

Despite the appealing geological character of pressure map, at this stage, care must be taken when comparing it with the flow simulator output. Understanding of pressure behavior is more incomplete than that of saturation and work with asset teams has to be done in order to validate such maps.

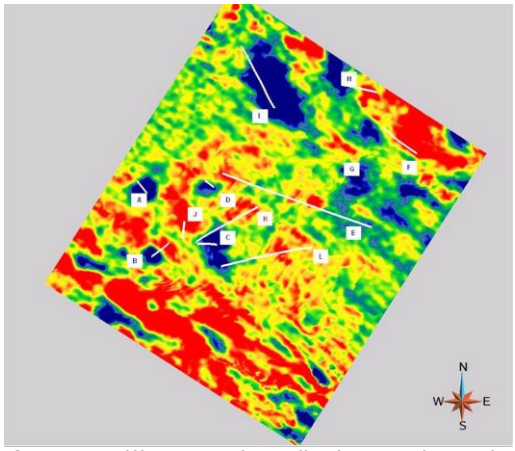

Figure 7: Difference of amplitude over the region of interest. Note the anomalies close to the wells.

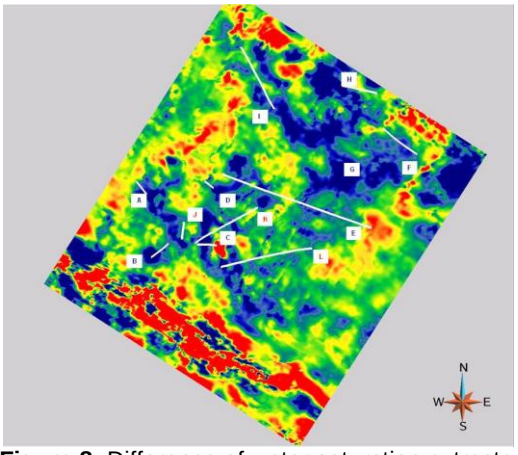

Figure 8: Difference of water saturation extracted on top reservoir. Anomalies remain close to the injector wells. Noise is smaller than in amplitude map, discarding the low coverage area in the bottom. Injectors in blue, producers in red, names at the bottom.

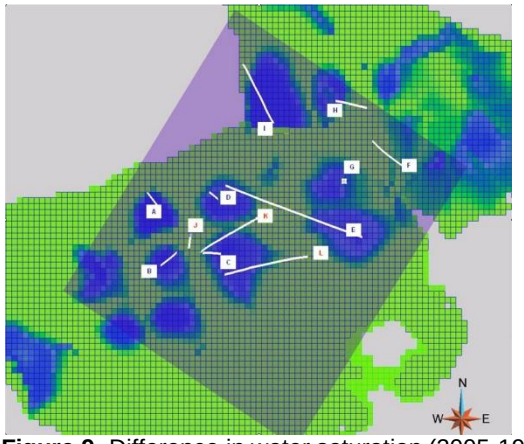

Figure 9: Difference in water saturation (2005-1997) from flow simulator.

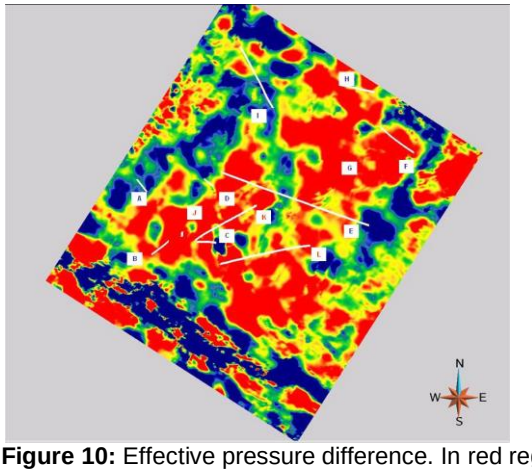

Figure 10: Effective pressure difference. In red regions were effective pressure is diminished due to increase in pore pressure caused by injection.

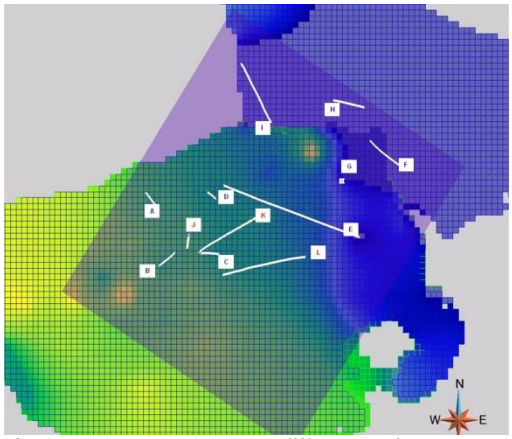

Figure 11: Pore pressure difference (2005-1997) predicted by flow simulator. Note that there is no evidence about the propagation of pressure changes near injector wells.

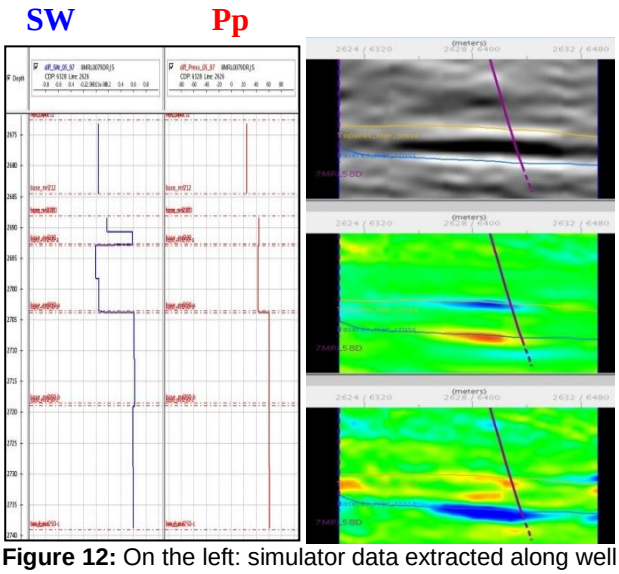

Figure 12: On the left: simulator data extracted along well path showing an increase in SW (blue) and pore pressure (red). On right side, section over the same injector well. From top: amplitude difference, saturation difference and effective pressure difference.

Another way to validate the anomalies is by making sections from the saturation / pressure differences volumes over some wells of interest and comparing with flow simulator data extracted along well path as shown in Figure 12. The simulator data on the left side show an increase in SW and pore pressure for the injector well **B**. In agreement with that, we see on the right the increase in water saturation and decrease of effective pressure, at the bottom of the reservoir. This validation was performed at all well locations and the results are listed on Table 1. Note the strong coherence between the two data.

Well	Pressure	Saturation
G	OK	OK
H	?	OK
F	OK	OK
J	OK	?
K	OK	?
I	?	OK
C	OK	OK
B	OK	OK
A	OK	OK
D	OK	OK

Table 1: Table showing the agreement or not between seismic data and flow Simulator data.

Conclusions

Despite the large uncertainty associated with the method, it has been possible, for this field, to obtain pressure and saturation change maps that correlate very well with flow simulator data (historically adjusted). The result is even better considering that no data other than seismic and petrophysical has been used. The main product is the qualitative understanding about the spreading of pressure changes within the reservoir, and how it is indiscernible in the amplitude map. Although we believe this map has a stronger geological character than the one from simulator, it is just the first step of a careful analysis to determine the pressure changes. This result is being currently analyzed by reservoir engineers to validate its accuracy.

We believe that future work, calibrating synthetic and real data, will allow quantitative predictions.

Acknowledgments

We acknowledge Petrobras Rock Physics group (G. Vasquez and J. Justen) for providing rock measurements and geophysicists Edgar Thedy and Marcos Grochau for useful comments. We also acknowledge Petrobras for the permission to present this paper.

References

Landro, M., 2001, Discrimination between pressure and fluid saturation changes from time-lapse seismic data, Geophysics, 66, 836-844.

MacBeth, C., Floricich, M. and Soldo, J., 2006, Going quantitative with 4D seismic analysis. Geophysical Prospecting, 54, 303-318.

Whitcombe, D.N., Dyce, M., McKenzie, C.J.S. and Hoeber, H., 2004, Stabilizing the AVO Gradient, SEG Expanded Abstracts, 23, 232.